OPENQUATERNARY

Mouchi, V, et al. 2020. Geochemistry of Bivalve Shells As Indicator of Shore Position of the 2nd Century BC. *Open Quaternary*, 6: 4, pp. 1–15. DOI: https://doi.org/10.5334/oq.65

RESEARCH PAPER

Geochemistry of Bivalve Shells As Indicator of Shore Position of the 2nd Century BC

Vincent Mouchi*, Laurent Emmanuel*, Vianney Forest† and André Rivalan‡

In an area named Mermian (municipality of Agde, South of France), a significant amount of fragmented italic amphorae from the 2nd century BC was discovered, located at a depth of 6 to 8 meters under the bed of the Hérault river. As no ship wreck was found in the vicinity, the reason of the presence of these amphora fragments, whose faces present a large accumulation of oyster shells, is unknown. Reconstructed geomorphological maps of the area present Mermian as a riverine site already at this period, and several hypothetical explanations on the role of these amphorae exist (landfill linked to a neighbouring habitat, bank reinforcement linked to a ford crossing, river landing, etc.). In order to define whether the amphorae were transported to this location and from where, we analysed the stable carbon and oxygen isotopes of the oyster shells. The $\delta^{13}C$ and $\delta^{18}O$ indicate that all oysters lived in the same environment, refuting a potential transport during the oyster accumulation. Moreover, the analysis of *Mytilaster* sp. shells in the sediment around the oyster shells also reported a marine origin, suggesting that these oysters were also buried in a marine deposit. Transport to Mermian from a coastal locality is unlikely but may still have happened, although no trace of human handling were observed on the fragments. Still, the presence of other marine or brackish molluscs in the sediment discards the interpretation of Mermian being a continental locality.

Keywords: *Ostrea edulis*; oyster shell; stable isotope; biomineralisation; Mermian; archaeology

Introduction

A dive carried out in 2004 as part of an archaeological survey of the Hérault river, led to the discovery in an area named Mermian (municipality of Agde, South of France) of a significant amount of fragmented italic amphorae located at a depth of 6 to 8 meters. This singular discovery, added to several testimonies of looting in its immediate surroundings, subsequently motivated the realization of several archaeological surveys between 2008 and 2009, followed in 2015 and 2016 by two campaigns consisting in the realization of test pits (Rivalan et al. 2017). At the end of the latter, it appeared that, despite the presence of actual traces of looting on the site, the initial hypothesis of an ancient boat wreck had to be rejected. The many test pits carried out indicate the existence of an important dump (18 m^2, 30–40 cm thick) of fragmented italic amphorae dating from the end of the 2nd century BC or the beginning of the 1st century BC, whose faces present a large accumulation of oyster shells. Despite these facts, the reasons for such an accumulation of ceramics in this part of the river remain highly uncertain (*i.e.*, landfill linked to a neighbouring habitat, bank reinforcement linked to a ford crossing, river landing, etc.).

The underwater site of Mermian is located in the heart of the lower Hérault valley, only five kilometers from the current Mediterranean coast (South of France; **Figure 1**). This vast alluvial plain is characterized by its borders consisting of ancient volcanic formations (Agde/Mont Saint-Loup and Saint-Thibéry) and alluvium from the Quaternary Period (Continental Pliocene), as well as its extensive continental and central filling linked to the floods of the Hérault river (Ambert 2001: 53–54). If this geographical context leads to the existence of areas systematically located in dry locations and provided with a good building material (*i.e.*, basalt), it also implies a major alluvial overlay and above all, numerous transformations of the landscape over time:

> 'If it is not possible to isolate within this sedimentation, in the absence of absolute dating or archaeological documentation, the sedimentary levels which belong to protohistory and antiquity, it is nonetheless permissible to conclude that the lower Hérault plain has undergone profound changes over time' (Ambert 2001: 54).

Taking these two characteristics into account therefore allows us to better understand the location of the antique sites associated with this geographical area, but also their near absence, all periods considered, along the Hérault river:

* Sorbonne Université, CNRS UMR 7193, ISTeP, F-75005, Paris, FR

† INRAP-Méditerranée, UMR 5068, TRACES, Toulouse, FR

‡ Université Paul Valéry–Montpellier 3, CNRS UMR 5140, ASM, Montpellier, FR

Corresponding author: Vincent Mouchi (vmouchi@gmail.com)

Figure 1: Localization of the Mermian site on the Mediterranean Sea coast, South of France. The reconstructed extension borders of the lagoons from the 2nd century BC are indicated in green (from Devillers et al. 2015).

> 'For the Gallo-Roman period, and especially during the Early Roman Empire, in view of the distribution map, one can speak of a strong anthropogenic pressure on the environment and in an agricultural context of full terroir. Only the banks of the Hérault river are empty of archaeological sites, but this is due to the mask of alluvial deposits: the only two points recognized are discoveries made at a depth of nearly 3 m, during powerful earthworks.' (Lugand & Bermond 2001: 93).

Although the alluvial overlay mentioned above (Ambert 2001: 54) logically implies an apparent absence of archaeological sites along the banks of the Hérault river, the immediate surroundings of Mermian nevertheless show traces of ancient occupation. Vestiges of an antique building dating back to the end of the 2nd century or the beginning of the 1st century BC has indeed been discovered about 500 meters northwest of the site at a depth of several meters (Lugand & Bermond 2001: 146). The presence of this building and above all its apparent contemporaneity with the underwater site of Mermian makes it therefore possible to imagine a relationship between these two sites, while providing a better understanding of the unearthed ceramics (*i.e.*, dump linked to the adjacent habitat or to a contemporary landing site, bank reinforcement intended to protect neighbouring agricultural parcels, or to consolidate a crossing system). That being said, the nature of this ceramic cluster, and especially the palaeoenvironment of the site, nevertheless raises a doubt as to the reasons that may have led to such an accumulation of ceramics in this particular location of the river.

The site of Mermian lies between 6 and 8 meters deep, and consists of a thick layer of clay, basalt blocks and ceramic fragments closely tangled. The latter have no particular organization and consist almost exclusively of fragmented italic amphorae and some elements belonging to the Dressel 1A type (Py 1993) which stems from the Italian Tyrrhenian coast and was largely produced between 135 and 50 BC. These fragments share not only similar dimensions and a relatively close level of entanglement, but also quasi-systematic remnants of pitch on their inner side, as well as many oyster shells (also present on the basalt blocks). The presence of pitch therefore allows us to deduce that these ceramics are derived from functional amphorae, while that of oysters implies their immersion in saltwater or brackish environment. Both left and right valves of these oysters are present, still attached on some specimens, which tends to indicate that these oyster-rich amphora fragments were not transported. However, numerous juvenile (<5 cm long) specimens are observed, mainly on late generations of oysters (*i.e.*, the juvenile specimens are attached to pre-existing full-grown right valves themselves attached to the amphora fragments). This observation may imply a change in the environment, towards less favourable conditions for oyster growth and survival, such as a riverine habitat. The accumulation of oyster shells on all visible faces of the ceramics (including the broken side) is also particularly interesting, since it tends to indicate the fixation of oyster spats and their growth within a cluster subjected to a powerful stream of salt water, or at least submitted to a low level of sedimentation. This last point is however somewhat problematic in that the work carried out through the DYLITAG project (Devillers et al. 2015, 2019) tends to show the remoteness of the riverine site from the lagoon of the time, and therefore an unfavourable environment for the accumulation of natural oysters. These various observations therefore raise doubt on the environmental conditions of Mermian at that time, and/or whether the amphora fragments were transported to this riverine location from the coastline.

Mollusc shells are ubiquitous remains amongst those found in archaeological sites (Bardot-Cambot 2014; Cariou et al. 2018; Forest 1998, 2003; Marchand et al. 2018). Multiple uses of these animals and their shells in various periods have been recognized (Claassen 1998)

and include food source (Waselkov 1987), ornamentation (Dupont, Hingant & Merle 2017; Ridout-Sharpe 2017), tool manufacture (Manca 2014; Szabó 2017), banking (Gruet 1993) and currency. Archaeologist can not only study the reason for their presence in specific sites, but also use sclerochronology (the shell equivalent to dendrochronology where each growth increment represents a specific time interval) to deduce the season of collection of studied specimens (Andrus 2011) and the ecology of known species to obtain information on the environment (Allen 2017). Moreover, the shells are made of calcium carbonate and they can also be used for absolute dating using radiocarbon method (Douka 2017; Fernandes & Dreves 2017). Last but not least, shell chemical composition can also hold substantial information regarding their living environment and the climate conditions (Andrus & Thompson 2012; Duprey et al. 2014; Harding et al. 2010).

As bivalve shells are built by the organism from chemical elements in its environment, the composition of the carbonate shell constituents can be used to reconstruct physicochemical settings of the living locality (Grimstead et al. 2013; Leng & Lewis 2016; Mouchi et al. 2018). In particular, the relative proportion of oxygen stable isotopes (compared to a standard value; $\delta^{18}O$) in biogenic carbonates are often used to reconstruct seawater temperature (Craig 1965). This temperature proxy is however challenging to interpret in coastal areas due to salinity fluctuations that also have an influence on the shell $\delta^{18}O$ through the seawater value of $\delta^{18}O$ ($\delta^{18}O_w$), which induces strong variations in shell $\delta^{18}O$ unrelated to temperature (Sharp 2007).

The ratio of carbon stable isotopes ($\delta^{13}C$) is generally more complex to interpret due to several potential factors of fluctuations in biogenic carbonates such as shells. Contrary to $\delta^{18}O$, $\delta^{13}C$ is not only influenced by environmental parameters, but also with metabolic processes that differ between species. In bivalve shells, $\delta^{13}C$ is influenced by: the dissolved inorganic carbon (DIC) which is naturally occurring in seawater; the $\delta^{13}C$ of the food source of the studied organism; and internal metabolic processes still not fully understood (Gillikin et al. 2006; Lartaud et al. 2010a; Riera & Richard 1996).

This study uses these isotope ratios as indicators of the living settings of the Mermian oysters for two purposes. Firstly, we wish to define if the specimens were transported at a time during their accumulation. Secondly, we discuss if they lived in an open marine location or in close proximity to a river output. A change in the isotopic composition of successive generations of shells would indicate a modification of the living settings for the organisms. We also compare these data with the isotopic signature of small bivalves found in the sediment around the amphorae to identify the *post-mortem* environmental conditions of the oysters.

Material and Methods

Modern hydrological context

The Mermian site is nowadays located beneath the Hérault river, which reaches the shore of the Mediterranean Sea over five kilometres downstream. The Hérault river represents one of the main reserves of freshwater of the region, with a mean rate of flow of 50 $m^3 \cdot s^{-1}$, along with periodic flooding of over 400 $m^3 \cdot s^{-1}$ (http://www.hydro.eaufrance.fr/). The Mediterranean Sea is a large enclosed basin with limited water input from the Atlantic Ocean through the Straits of Gibraltar, which induces a very low tide (a few centimetres, compared to metric range in the Atlantic Ocean; McElderry, 1963). This particularity of the Mediterranean Sea prevents the tidal-influenced flooding of the lower part of the Hérault river, and salinity is therefore kept low across the entire stream. The seawater temperature of this area ranges from 12 to 23°C throughout the year (www.meteociel.fr). Temperature of the Hérault water ranges from 13 to 25°C from April to July (www.naiades.eaufrance.fr) and down to 6°C from December to February (observations from diving computer; Rivalan, personal communication). Salinity from measurements at the Florensac station (located approx. 2 km upstream Mermian on the Hérault river) is 0.1‰ (www.naiades.eaufrance.fr). The current malacofauna of the Hérault river reflects that low salinity (*e.g.*, *Dreissena*, *Sinanodonta woodiana*). The mean salinity along the French Mediterranean coastline is 37.5‰.

Specimen preparation

In order to define the living environment of the oysters and if it changed during the accumulation of successive generations (such as if the oysters were transported), multiple specimens (some attached to amphorae and some attached to pre-existing generations of oysters; **Figure 2a**) were analysed to maximize the chances of obtaining specimens which could have lived in different environments.

All specimens were cleaned from their surrounding sediment under tap water. Several specimens of the mussel

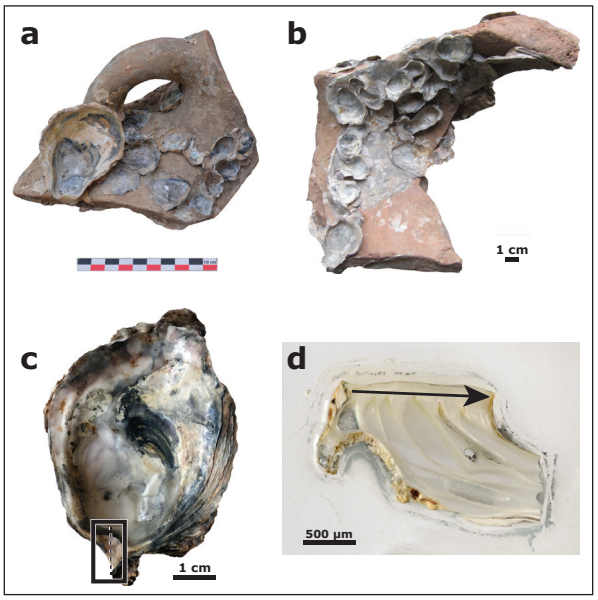

Figure 2: Preparation of Mermian oyster shells. **a–b:** Oyster shells attached to amphora fragment with some successive generations (see upper part of b). **c:** Oyster shell showing the umbo region of the left valve. The dashed line represents the cut direction for a section. **d:** Section of the umbo region. The arrow indicates the growth direction on the pristine foliated carbonate microstructure.

Mytilaster sp. (rarely holding both valves) were found during this process. Oyster shells were then cleaned from epibionts (barnacles) using a Dremel. The umbo region of the left valves, holding the complete and condensed accumulation of carbonates formed during the entire shell growth (Kirby, Soniat & Spero 1998; Lartaud et al. 2010b), were subsequently cut and embedded in Huntsman Araldite 2020 to ensure the physical preservation of the structures (**Figure 2b–c**). The umbo regions were cut along the maximum growth axis (through the middle of the hinge region to the ventral shell margin). The two resulting halves of each umbo were used to make thin sections and isotopic sampling. Thin sections were used for microscope and cathodoluminescence observations to ensure the pristine state of the shells and to obtain a seasonal-scale temporal calibration (Langlet et al. 2006; Mouchi et al. 2018). Cathodoluminescence observations were performed on a Cathodyne OPEA cold cathode with operating settings of 15–20 kV and 200–400 $\mu A \cdot mm^{-2}$. Specimens exhibiting suspicious microtextural patterns were discarded. Intensity of luminescence (in arbitrary units) were obtain along a continuous transect using the NIH-ImageJ software (ver. 1.52a) and high values were considered to correspond to parts of the umbo formed during summer periods (**Figure 3**). More precisely, substantial drops of luminescence on the profiles were assumed to correspond to the middle of a winter period. Verification was made on the pictures (**Figure 3a**) for each of these assumed positions, as bias may occur depending on the trajectory of the selected transect on ImageJ. In such cases, modifications of the positions of winter periods were made from visual observations of luminescent bands. As a confirmation, a second seasonal calibration method from Kirby, Soniat & Spero (1998) was attempted. This technique uses a sclerochronological record on the ligamental area in the form of external convex and concave bands. Unfortunately, umbos from these specimens did not exhibit the necessary curved surface to conduct such a study.

Isotope measurements

A total of 13 specimens were selected from their preservation state for stable isotope analysis. Successive samples were collected from the remaining half of the umbo region (*i.e.*, the half not used for thin section) of each specimen to obtain a minimum of 40 μg of carbonate powder per sample using a dentist drill with a 0.5 mm burr. Positions of the samples were chosen to cover the extrema of cathodoluminescence intensity (*i.e.*, summer and winter periods) in order to get the maximum amplitude of seasonal temperature contrasts. Cathodoluminescence seasonal calibration was checked on specimen M2 by performing isotope analysis on an extended profile. Variations of $\delta^{18}O$ follow the seasonal model as expected, with low and high isotopic values corresponding to high and low values of cathodoluminescence intensity, respectively. Note that for specimen M1, 11 samples were collected and analysed but only eight are in the range of the cathodoluminescence analysis of the corresponding thin section. Juvenile shells could not be analysed due to the extremely thin foliated calcite available on the umbo region (<0.1 mm thick; Supplementary Information 1) which could not be sampled without contamination from the resin and the external edge of the shell. Moreover, a sample from a *Mytilaster* sp. specimen found in the sediment surrounding the oyster shells was collected. The very fragile shell of this species prevented multiple successive sampling following

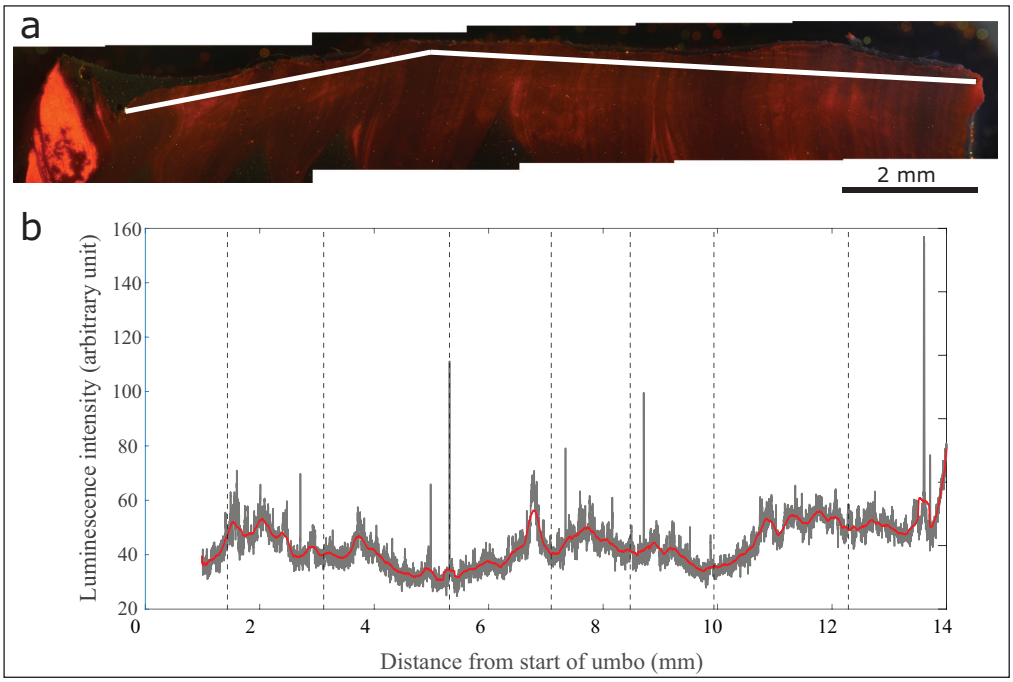

Figure 3: Seasonal calibration of the umbo region of an oyster shell from cathodoluminescence. **a:** Cathodoluminescence image of the umbo region of an oyster shell (as shown on Figure 1c). **b:** Intensity of luminescence (with moving average) taken from a transect following growth (white line on a). The vertical dashed lines represent the positions of the winters. This specimen is interpreted to be 8 years old at the time of its death.

growth structures, and a bulk sampling strategy was used instead.

Analyses were performed at Sorbonne Université (Paris, France) using a Kiel IV carbonate device and a DELTA V isotope ratio mass spectrometer by measuring the oxygen and carbon stable isotopes of carbon dioxide generated by the dissolution of samples using anhydric orthophosphoric acid at 70°C (McCrea 1950). Isotope values are reported in delta (δ) notation, relative to Vienna Peedee Belemnite. Accuracy and precision of 0.08‰ (1 σ) were determined by repeated analyses of a marble working standard, calibrated against the international standard NBS-19.

Results

Stable isotopes

Oxygen stable isotope ratios range from −1.55 to 2.14‰ (VPDB) (**Figures 4** and **5**, **Table 1**). Multiple comparison procedure indicates that the range of these values is not statistically different for all specimens (Tukey test, $p > 0.14$).

Carbon stable isotope ratios present values between −1.84 and 0.33‰ (VPDB) (**Figures 4** and **5**, **Table 1**). Tukey test does not report statistically different populations between all specimens ($p > 0.84$).

Correlations between $\delta^{18}O$ and $\delta^{13}C$ for all specimens, except specimen M6, are non-significant positive or negative correlations, depending on the specimens. Specimen

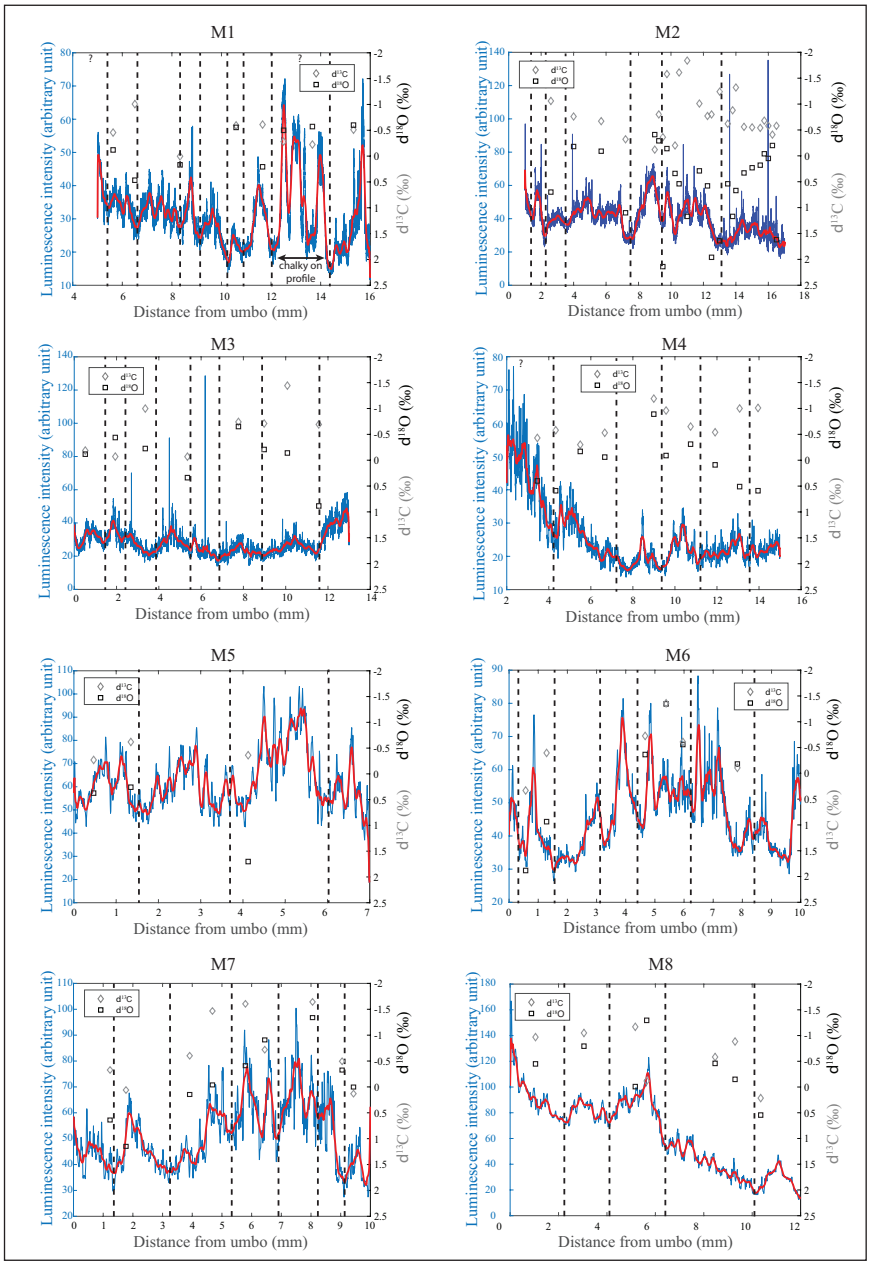

Figure 4: Carbon (grey diamonds) and oxygen (black squares) stable isotope ratios of specimens M1 to M8 with intensity of cathodoluminescence profiles (in blue, with smoothed signal in red for clarity). The abscissa represents the positions of cathodoluminescence intensity and isotope samples along the umbo region of each specimen, with the origin as the apex. The cathodoluminescence profile of specimen M1 passes through chalky structures which artificially induce high intensity of luminescence unrelated to season. Positions of interpreted winter extrema from cathodoluminescence are indicated by dashed vertical lines.

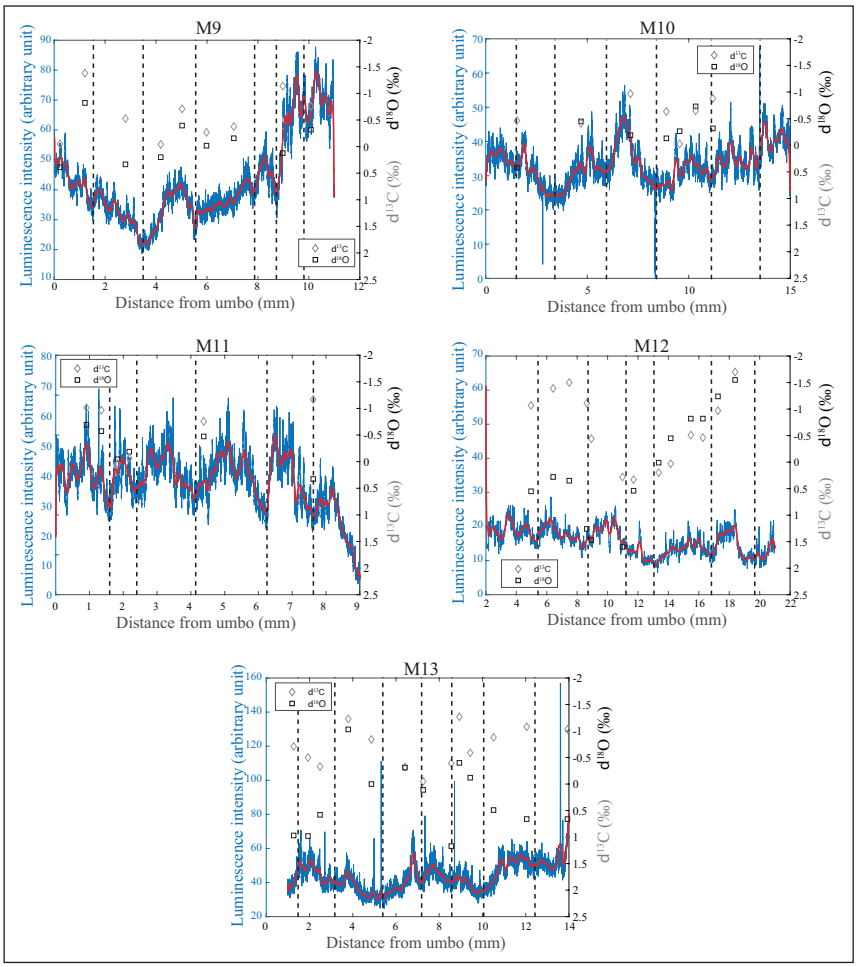

Figure 5: Carbon (grey diamonds) and oxygen (black squares) stable isotope ratios of specimens M9 to M13 with intensity of cathodoluminescence profiles (in blue, with smoothed signal in red for clarity). The abscissa represents the positions of cathodoluminescence intensity and isotope samples along the umbo region of each specimen, with the origin as the apex. Positions of interpreted winter extrema from cathodoluminescence are indicated by dashed vertical lines.

Table 1: Stable isotopes from the Mermian oyster shells.

Sample	Position (mm)	$\delta^{13}C$ (‰ VPDB)	$\delta^{18}O$ (‰ VPDB)
M1	5.6	−0.46	−0.12
	6.5	−1.01	0.47
	8.3	0.00	0.17
	10.6	−0.59	−0.56
	11.7	−0.61	0.21
	12.5	−0.28	−0.50
	13.7	−0.22	−0.57
	15.3	−0.51	−0.60
M2	2.6	−1.06	0.70
	4.0	−0.76	−0.18
	5.7	−0.67	−0.09
	7.2	−0.32	1.10
	9.0	−0.12	−0.41
	9.25	−0.80	−0.29
	9.5	−0.36	2.14
	9.75	−1.58	−0.14

(Contd.)

Sample	Position (mm)	$\delta^{13}C$ (‰ VPDB)	$\delta^{18}O$ (‰ VPDB)
	10.25	−0.20	0.34
	10.5	−1.61	0.54
	11.0	−1.84	1.17
	11.75	−1.01	0.29
	12.25	−0.77	0.58
	12.5	−0.80	1.96
	13.0	−1.24	1.64
	13.5	−0.62	0.54
	13.8	−0.88	1.17
	14.0	−1.32	0.67
	14.5	−0.56	0.33
	15.0	−0.55	0.23
	15.5	−0.54	0.18
	15.75	−0.68	−0.04
	16.0	−0.58	0.05
	16.25	−0.41	−0.20
	16.5	−0.58	1.62
M3	0.5	−0.19	−0.12
	1.9	−0.07	−0.44
	3.4	−1.00	−0.23
	5.4	−0.07	0.34
	7.8	−0.74	−0.65
	9.0	−0.71	−0.21
	10.1	−1.44	−0.14
	11.6	−0.69	0.89
M4	3.5	−0.43	0.40
	4.3	−0.58	0.59
	5.5	−0.30	−0.17
	6.7	−0.53	−0.06
	9.0	−1.19	−0.89
	9.6	−0.96	−0.09
	10.7	−0.65	−0.31
	11.9	−0.54	0.09
	13.1	−1.00	0.51
	14.0	−1.01	0.59
M5	0.5	−0.27	0.37
	1.3	−0.62	0.26
	4.1	−0.36	1.70
M6	0.6	0.33	1.88
	1.3	−0.40	0.94
	4.7	−0.72	−0.36
	5.4	−1.36	−1.35
	6.0	−0.61	−0.56
	7.8	−0.11	−0.18

(Contd.)

Sample	Position (mm)	$\delta^{13}C$ (‰ VPDB)	$\delta^{18}O$ (‰ VPDB)
M7	1.2	–0.33	0.64
	1.7	0.06	1.15
	3.9	–0.60	0.15
	4.6	–1.47	–0.04
	5.7	–1.61	–0.41
	6.4	–0.72	–0.91
	8.0	–1.65	–1.34
	9.0	–0.50	–0.33
	9.4	0.13	0.00
M8	1.0	–0.97	–0.45
	3.1	–1.05	–0.79
	5.2	–1.17	–0.01
	5.6	–0.12	–1.30
	8.5	–0.58	–0.46
	9.3	–0.88	–0.15
	10.4	0.22	0.54
M9	0.2	–0.05	0.39
	1.2	–1.38	–0.82
	2.8	–0.52	0.33
	4.2	–0.04	0.20
	5.0	–0.71	–0.40
	6.0	–0.27	–0.02
	7.1	–0.38	–0.16
	9.0	–1.14	0.12
	10.1	–0.76	–0.32
M10	1.5	–0.43	0.42
	4.7	–0.38	–0.45
	7.1	–0.94	–0.19
	8.9	–0.61	–0.13
	9.6	0.00	–0.26
	10.3	–0.65	–0.73
	11.2	–0.88	–0.32
M11	0.9	–1.01	–0.69
	1.4	–0.97	–0.57
	1.8	0.04	–0.04
	2.2	–0.07	–0.19
	4.4	–0.76	–0.47
	7.6	–1.17	0.33
M12	5.0	–1.07	0.55
	6.4	–1.39	0.28
	7.5	–1.50	0.35
	8.6	–1.11	1.26
	8.9	–0.44	1.47
	11.0	0.28	1.60

(Contd.)

Sample	Position (mm)	$\delta^{13}C$ (‰ VPDB)	$\delta^{18}O$ (‰ VPDB)
	11.7	0.33	0.54
	13.4	0.20	0.01
	14.2	0.03	–0.45
	15.5	–0.51	–0.82
	16.3	–0.46	–0.82
	17.3	–0.97	–1.24
	18.4	–1.70	–1.55
M13	1.3	–0.71	0.97
	1.9	–0.50	0.98
	2.5	–0.33	0.58
	3.8	–1.23	–1.03
	4.9	–0.84	0.00
	6.4	–0.32	–0.31
	7.3	–0.05	0.11
	8.6	–0.39	1.17
	8.9	–1.27	–0.40
	9.4	–0.59	–0.12
	10.5	–0.88	0.49
	12.0	–1.08	0.66
	13.9	–1.03	0.66

M6 presents a significant positive correlation between $\delta^{18}O$ and $\delta^{13}C$ ($p = 0.03$).

The bulk analysis of the *Mytilaster* sp. specimen indicated a mean $\delta^{18}O$ of 0.83‰ (VPDB) and $\delta^{13}C$ of 0.09‰ (VPDB).

Growth rates of oyster shells

The smoothed intensity of luminescence (using a moving average; **Figures 4** and **5**) allows the estimation of age for each specimen at the time of death. The resulting age models gave lifespans for each individual oyster between 3.5 and 9 years. These ages were compared to the total size of the shell in order to obtain the mean growth rate for each specimen. The mean shell growth rate for all specimens (**Figure 6**) follow a linear distribution. The data were tested for outliers (considering an outlier is more than three scaled median absolute deviations (MAD) away from the median) which could be interpreted as a significantly different growth rate which could be reflecting different environmental settings. No outlier was detected.

Discussion

The isotopic composition of the shells allows to obtain information on the living environment of oysters. Although absolute values cannot be properly compared between localities due to differences in seawater and freshwater $\delta^{18}O$, **Figure 7a** presents datasets from various environments exhibiting characteristic dispersion of values. In close proximity and influence of a river output, the freshwater induces a depletion in $\delta^{18}O_w$ and thus shell $\delta^{18}O$ as well as occasionally large amplitude of values (*i.e.*, estuarine from Walther & Rowley 2013; **Figure 7a**). Alternatively, in locations without direct freshwater input such as open marine settings, $\delta^{18}O$ fluctuations are governed by temperature variations (*i.e.*, marine from Tynan et al. 2014; Walther & Rowley 2013; **Figure 7a**). The $\delta^{13}C$ is however challenging to interpret. It has been demonstrated that the carbon isotopic composition from oyster shells fluctuates with the dissolved inorganic carbon in the water, the food source and metabolic processes (Gillikin et al. 2006; Lartaud et al. 2010a; McConnaughey & Gillikin 2008), and the comparison of data from a selection of publications on **Figure 7a** (Surge & Lohmann 2008; Tynan et al. 2014; Walther & Rowley 2013) indeed illustrates the potential influence of several parameters. Inter-specific differences cannot be the major factor as *Crassostrea virginica* exhibits distinct $\delta^{13}C$ in Florida (Surge & Lohmann 2008) and Texas (Walther & Rowley 2013). Local conditions therefore control the shell $\delta^{13}C$, whether from the dissolved inorganic carbon or the food source. It is known that particulate organic carbon is generally enriched in ^{13}C (less negative $\delta^{13}C$) from riverine to marine environments (Hughes & Sherr 1983; Incze et al. 1982; Riera & Richard 1996). The 95% confidence intervals of the distributions of the various estuarine datasets in **Figure 7a** tend to follow this behaviour, with not only larger amplitude of $\delta^{13}C$, but also with more negative $\delta^{13}C$ values associated with depleted oxygen composition (reflecting lower salinity in those environments) due to freshwater input, with different food source for the oysters compared to marine water.

The shape of these 95% confidence intervals tends to be a vertically-oriented ellipse with restricted amplitudes of both isotopic ratios for open marine settings (without significant correlation between $\delta^{13}C$ and $\delta^{18}O$; in magenta and dark blue on **Figure 7a**), and is a larger-amplitude

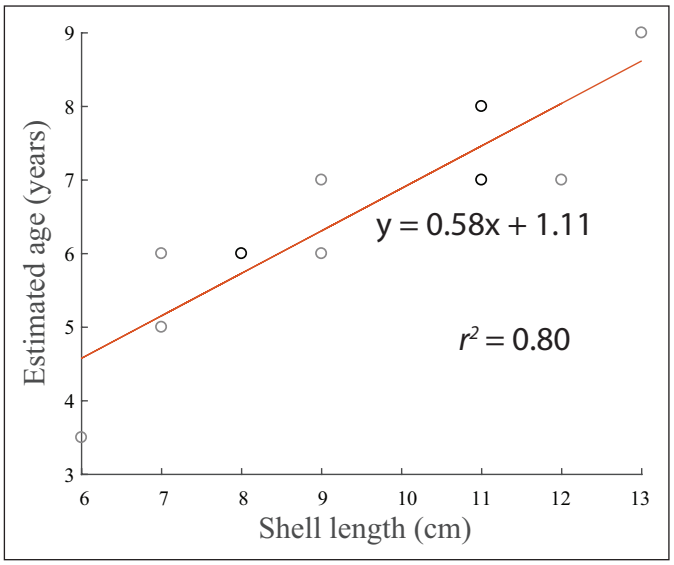

Figure 6: Regression relation between shell length and estimated age from cathodoluminescence profiles. Black dots correspond to superimposition of two observations.

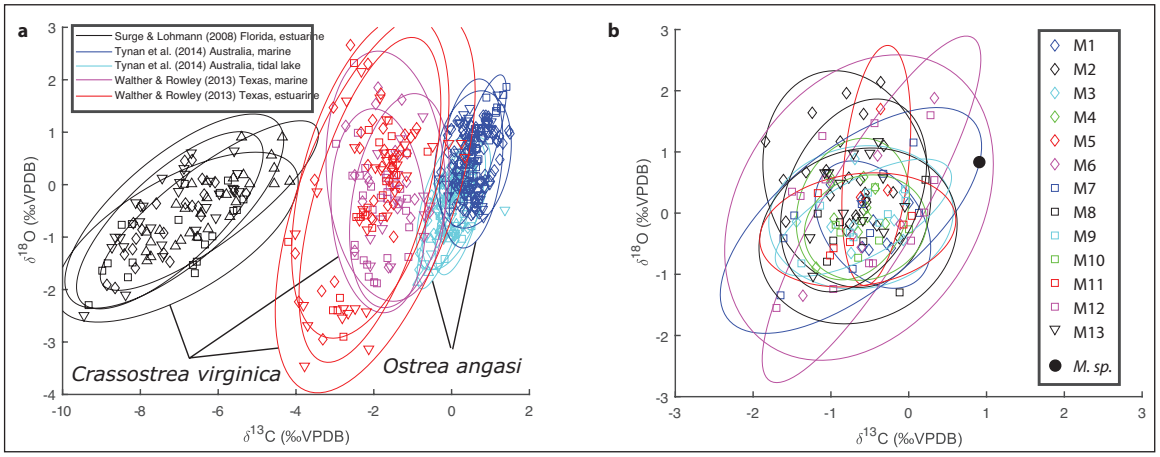

Figure 7: Oxygen and carbon stable isotopes from oyster shells in different environmental settings for distribution comparison. Each domain from this figure encloses the 95% confidence interval error ellipse of the distribution of carbon and oxygen isotopes from multiple measurements along the shell of several specimens. **a:** Selected modern environments from the literature, corresponding to estuarine and open marine. Estuarine environments correspond to positive correlation patterns (tilted ellipses) while open marine localities present no significant correlation. **b:** Mermian specimens. For comparison, the large black dot indicates the bulk isotopic composition of a *Mytilaster* sp. shell found in the sediment surrounding the oysters at Mermian.

diagonally-oriented ellipse for estuarine environments (corresponding to a highly significant positive correlation between both stable isotope ratios; $p < 0.01$, in cyan, black and red on **Figure 7a**). The shapes of the distributions of Mermian specimens (**Figure 7b**) are not as clear as the other distributions from the literature, although no significant correlation has been found on most specimens between $\delta^{13}C$ and $\delta^{18}O$. Most Mermian specimens mainly correspond to open marine distribution with some specimens showing slightly tilted ellipses (*i.e.*, M6, M7, M9). The only specimen exhibiting a significant positive correlation is specimen M6. This specimen was one of those directly attached to an amphora fragment. Although a definite relative chronology of the accumulated specimens is impossible due to probably numerous successive generations of oysters, such position of the specimen should indicate that it predates at least some other specimens. This is also the case for specimen M7, which also exhibits a non-significant positive correlation. This would argue against the interpretation, by taking in consideration only these observations, of a change of environment chronologically from an open marine setting to a closer proximity to a river output, but rather the opposite. Also, the amplitude of both isotope ratios are not higher than those of other specimens, contrary to what is observed in the literature between open marine and estuarine localities (**Figure 7a**).

The observed distributions of all Mermian isotopic data tend to indicate that most specimens did not live in direct proximity to a river output, as observed for the data presented in **Figure 7a** (Surge & Lohmann 2008; Tynan et al. 2014; Walther & Rowley 2013) and from other data collected on oyster shells from various coastal areas of

France (Lartaud, 2007). It is however possible that this can be due to missing data during low temperature and/or salinity periods. Indeed, interspecific differences on the temperature and salinity tolerance may be at play, with *O. edulis* unable to build shell increments in lower salinity settings. This way, no shell carbonate could be sampled for isotopic analysis to obtain the complete record of the environment. This assumption has been advanced by Surge and Lohmann (2008) to explain the range of $\delta^{18}O$ of their specimens, which is lower than expected considering the large salinity variations observed on site. If *O. edulis* specimens would have experienced low salinity conditions and been able to produce shell increments, additional data would probably be present on **Figure 7b** at the bottom left corner of Mermian distributions, where $\delta^{18}O$ (for low salinity) and $\delta^{13}C$ (for food from continental origin) would be lower than presently represented, and the distribution would have a shape of diagonally-oriented ellipse with significant positive correlation.

By considering there was no transport of the amphora fragments (and thus of the oysters), we can reconstruct temperatures from the $\delta^{18}O$ of specimens M6 and M12, which present the largest range of values (**Figures 4** and **5**), and two possible values of $\delta^{18}O_w$ have to be tested: a seawater value and an estuarine value. To do this, we used the equation of Pierre (1999) set up in the Mediterranean Sea and linking salinity to $\delta^{18}O_w$ with salinity values of 37.5 and 22‰ for the Mediterranean Sea and a value corresponding to the minimum salinity for which *O. edulis* can grow (Marteil 1960; His 1968), respectively (see first section of the Material and Methods). We obtained $\delta^{18}O_w$ of 1.23 and –2.96‰ for the Mediterranean Sea and the low salinity setting, respectively. Using these values in the temperature reconstruction model from shell $\delta^{18}O$ of Anderson and Arthur (1983), we obtained temperatures from specimen M6 ranging from 13.3 to 27.5°C and from –1.0 to 9.6°C for a Mediterranean Sea and a low salinity setting, respectively, and for specimen M12 from 14.5 to 28.5°C and from –0.2 to 10.4°C for a Mediterranean Sea and a low salinity setting, respectively. The lower limit of the Mediterranean Sea interpretation is similar to modern values (12°C; www.meteociel.fr), but the upper limit is 4 to 5°C higher than modern observations (23°C; www.meteociel.fr). Lower salinities can overestimate reconstructed temperatures, but the largest difference compared to modern values occurs in summer, while flooding from the Hérault river generally happen during autumn and winter months. It is also possible that the South of France during the 2nd century BC was subject to higher summer temperatures than today, although Luterbacher et al. (2016) reconstructed similar climate at this time compared to present. The values interpreted from the low salinity $\delta^{18}O$ are systematically aberrant, which confirm the impossibility of growth in direct proximity of the river output. Another test can be performed by considering a mean salinity of 35‰ (corresponding to an environment nearby a river output in the Mediterranean Sea), which, using the same equations cited above, would give a $\delta^{18}O_w$ of 0.55‰ and reconstructed temperatures ranging from 10.7 to 24.3°C and from 11.8 to 25.3°C for specimens M6 and M12, respectively. These values are more in accordance to the expected temperature range. In absence of transport of the shells, the isotopic data are thus in direct opposition to the reconstructed map of the area corresponding to the 2nd century BC (Devillers et al. 2015, 2019), which indicates that Mermian was already a fluvial locality at this period.

A possible explanation to this discrepancy is the hypothesis that the amphorae (and the oyster shells) were transported to Mermian from a coastal location further South. Oyster aquaculture, and the related transport of the amphorae fragments, was the starting point of this study for it would have provided an appropriate explanation to the presence of the oyster cluster at this precise location. Antique sources do tend to indicate that oyster growth on ceramic fragments had already been observed at that time (Brien-Poitevin 1996, p. 317 and Bardot-Cambot and Forest 2013, p. 373–374), but no archaeological evidence supports that this knowledge was used to get "oysters to eat" in the way of modern oyster farming (Bardot-Cambot and Forest 2013). The only elements which can be related to oyster farming are representations of *Ostriaria* on glass vases of Baies (Campania) dating back to the 3rd and 4th century AD (https://arachne.dainst.org – Cologne University, objects number 608604, 608598 and 608586), however the precise function of the wooden structures figured still remains uncertain (*i.e.*, oyster refining structures or real breeding supports; Bardot-Cambot and Forest 2013, p. 377–378). Moreover, the use of ceramics during the 2nd century BC would be too early as the large consumption and selling of oysters only started in the few years prior to the common era in the region (Bardot-Cambot and Forest 2014). Transport for (or due to) aquaculture is therefore discarded.

Although the apparent large proportion of juvenile shells amongst the latest generations of oysters (which could have been interpreted as an environmental change less favourable for oyster development, such as a riverine site), the homogeneity of the isotopic composition between specimens indicates that all specimens have lived in the same coastal environment, therefore no evidence of transport during the growth of the oyster generations can be found. The growth rate measurements (**Figure 6**) also confirm the same environmental conditions, as it has been shown that local settings induce differences in growth rates from one locality to another (Lartaud et al. 2010c). Moreover, the bulk sample of *Mytilaster* sp. also presents a marine isotopic signature with a positive $\delta^{18}O$ (**Figure 7b**) which coincides with the known ecology of this taxon restricted to marine and brackish environments (MolluscaBase 2019a). Indeed, a freshwater $\delta^{18}O$ signature would be represented by a strongly negative value (Pfister et al. 2019) and estuarine environments would be represented by intermediate values. This tends to prove that both *O. edulis* ($\delta^{18}O$ between –2 and 2‰) and *Mytilaster* sp. ($\delta^{18}O \approx 1$‰) lived by the shore and not in direct proximity to the river output. The presence of marine *Mytilaster* sp. in the sediment directly surrounding the amphorae indicates that these bivalves lived there contemporaneously and probably after the oysters. This observation implies that these sediments correspond to

marine (or at least coastal) deposits after the burial of the amphorae and the oysters. Some *Cerastoderma* shells (known to live in brackish and marine environments; MolluscaBase 2019b) were found in the sediment of the same stratigraphic unit (Rivalan et al. 2017). It is possible that these specimens lived in a lagoon and that the amphorae were transported there. These organisms are however not able to survive in freshwater, and the interpretation of a fluvial dump site (or bank reinforcement linked to a ford crossing) is challenged. Moreover, as the sediment around the oyster shells (and the amphorae) was very easily removed under tap water also argues against a transport to a fluvial environment as the consequent rate of flow of the Hérault river would have washed away this sediment and the *Mytilaster* sp. shells. In order to indicate whether the amphorae fragments were transported from the shore to a lagoon, a more comprehensive study of the sediment, involving particle size analysis and mineralogical assemblage, would be required on sediment cores in order to note potential changes within the stratigraphic unit holding the amphorae and the various bivalve species presented here.

If an anthropic transport of these amphorae has indeed happened, it appears that these fragments were moved not only along with the oysters after their death but also with a substantial amount of surrounding sediment hosting the *Mytilaster* sp. shells (that somehow resisted to the rate of flow of the Hérault river) and the basalt blocks from a coastal locality (maybe nearby a river output) to a lagoon, where the *Cerastoderma* could be an indicator. No evidence of handling of the amphora fragments (*i.e.*, broken pieces of the ceramics and the shells) were observed, which tends to refute this hypothesis. The alternative hypothesis would involve to challenge the reconstructed geomorphological map (Devillers et al. 2015, 2019) by considering the Mermian site as a coastal area with the Hérault river reaching the shore at a nearby location. In any case, no evidence of fluvial settings was found in the malacological assemblage observed from the amphora fragments accumulation.

Conclusion

This study presented an application of stable isotopes as a means to indicate a change in the living environment of mollusc species attached to amphora fragments. The isotope results are in accordance to the setting reconstruction from the assemblage. Our results refute the hypothesis of a transport of these amphorae during the growth of the oysters and contradict the reconstructed geomorphological map of the area during the 2nd century BC.

The presence of the amphora fragments there remains to be explained, but it appears that any previous interpretation considering a continental setting (such as landfill linked to a neighbouring habitat, bank reinforcement linked to a ford crossing, and river landing) have to be discarded. Our results indicate a lagoon or an estuarine setting, with clear marine influence, at Mermian during the studied period.

Although a definite answer has not yet been provided regarding the anthropic transport of the amphora fragments, this work highlights the benefits of mollusc shell geochemistry as a tool for palaeoenvironmental reconstructions when combined with the archaeologic reasoning in marine and coastal settings.

Additional File

The additional file for this article can be found as follows:

- **Juvenile shell description.** Structures are too narrow for sampling. DOI: https://doi.org/10.5334/oq.65.s1

Acknowledgements

The authors wish to thank Nathalie Labourdette, Léa Beaumont, Zoélie Gourves-Nurit and Marie Pesnin for their help with the sampling and IRMS analysis of carbonate powder. We also thank two anonymous reviewers for their thorough comments which significantly helped to improve the clarity of the final version of the manuscript.

Competing Interests

The authors have no competing interests to declare.

Author Contributions

A.R. and V.F. provided the shells and led the archaeological impact on the study. V.M. and L.E. provided expertise on the geochemistry. All authors contributed to the writing of the manuscript.

References

Allen, MJ. 2017. Land snails in archaeology. In Allen, MJ (ed.) *Molluscs in Archaeology*. Oxford: Oxbow Books. 6–29. DOI: https://doi.org/10.2307/j.ctvh1dk5s.7

Ambert, P. 2001. Géologie et géomorphologie des pays de l'étang de Thau et de la basse vallée de l'Hérault. In: *Carte Archéologique de la Gaule : Agde et le Bassin de Thau*, 34/2, 48–57. Paris: Académie des Inscriptions et Belles-Lettres – Maison des Sciences de l'Homme.

Anderson, TF and **Arthur, MA.** 1983. Stable isotopes of oxygen and carbon and their application to sedimentologic and paleoenvironmental problems. In: Arthur, MA, Anderson, TF, Kaplan, IR, Veizer, J and Land, L (eds.), *Stable isotopes in sedimentary geology*, S.E.P.M., Short Course, 1–151. DOI: https://doi.org/10.2110/scn.83.01.0000

Andrus, CFT. 2011. Shell midden sclerochronology. *Quaternary Science Reviews*, 30: 2892–2905. DOI: https://doi.org/10.1016/j.quascirev.2011.07.016

Andrus, CFT and **Thompson, VD.** 2012. Determining the habitats of mollusk collection at the Sapelo Island shell ring complex, Georgia, USA using oxygen isotope sclerochronology. *Journal of Archaeological Science*, 39: 215–228. DOI: https://doi.org/10.1016/j.jas.2011.08.002

Bardot-Cambot, A. 2014. Coquillages des villes et coquillages des champs : une enquête en cours. In: Deru, X and Gonzalez Villaescusa, R (eds.), *Consommer dans les campagnes de la Gaule Romaine*, 21: 109–123. Lille: Revue du Nord SI, Collection Art et Archéologie.

Bardot-Cambot, A and **Forest, V.** 2013. Ostréiculture et mytiliculture à l'époque romaine ? Des définitions modernes à l'épreuve de l'archéologie. *Revue archéologique*, 2013/2(56): 367–388. DOI: https://doi.org/10.3917/arch.132.0367

Bardot-Cambot, A and **Forest, V.** 2014. Une histoire languedocienne des coquillages marins consommés, du Mésolithique à nos jours. In: Costamagno, S (ed.) *Histoire de l'alimentation humaine : entre choix et contraintes*. Actes du 138e Congrès national des sociétés historiques (Rennes, 2013), 88–104. Paris: Éditions du CTHS.

Brien-Poitevin, F. 1996. Consommation des coquillages marins en Provence à l'époque romaine. *Revue archéologique de Narbonnaise*, 29: 313–320. DOI: https://doi.org/10.3406/ran.1996.1478

Cariou, E, Baltzer, A, Leparoux, D, Ledoyen, J and **Debaine, F.** 2018. Ground penetrating radar in the medieval oyster shell middens of Saint-Michel-en-l'Herm (Vendée, France). *Journal of Archaeological Science: Reports*, 18: 186–196. DOI: https://doi.org/10.1016/j.jasrep.2017.12.048

Claassen, C. 1998. *Cambridge Manuals in Archaeology: Shells*. Cambridge: Cambridge University Press.

Craig, H. 1965. The measurement of oxygen isotope palaeotemperatures. In: Tongiori, E (ed.), *Stable isotopes in oceanographic studies and palaeotemperatures*, 161–182. Pisa: Consiglio Nazionale delle Ricerche Laboratorio di Geologia Nucleare.

Devillers, B, Bony, G, Degeai, J-P, Gasco, J, Lachenal, T, Bruneton, H, Yung, F, Oueslati, H and **Thierry, A.** 2019. Hoocene coastal environmental changes and human occupation of the lower Hérault River, southern France. *Quaternary Science Reviews*, 222: 105912. DOI: https://doi.org/10.1016/j.quascirev.2019.105912

Devillers, B, Bony, G, Degeai, J-P, Gasco, J, Oueslati, H, Bermond, I and **Yung, F.** 2015. Coastal and human settlement in the lower Hérault river (Southern France) since the Neolithic: environment – human society interactions in holocene mediterranean. In: XIX INQUA Congress, Quaternary Perspectives on Climate Change, Natural Hazards and Civilisation, 26 July–2 August 2015, Nagoya, Japon.

Douka, K. 2017. Radiocarbon dating of marine and terrestrial shell. In: Allen, MJ (ed.), *Molluscs in Archaeology*, 381–399. Oxford: Oxbow Books. DOI: https://doi.org/10.2307/j.ctvh1dk5s.28

Dupont, C, Hinguant, S and **Merle, D.** 2017. Diversité des territoires d'origine des parures en coquillages mésolithiques de la grotte Rochefort (Saint-Pierre-sur-Erve, Mayenne). *Bulletin de la Société préhistorique française*, 114(1): 7–23.

Duprey, N, Galipaud, J-C, Cabioch, G and **Lazareth, CE.** 2014. Isotopic records from archeological giant clams reveal a variable climate during the southwestern Pacific colonization ca. 3.0 ka BP. *Palaeogeography, Palaeoclimatology, Palaeoecology*, 404: 97–108. DOI: https://doi.org/10.1016/j.palaeo.2014.04.002

Fernandes, R and **Dreves, A.** 2017. Bivalves and radiocarbon. In: Allen, MJ (ed.), *Molluscs in Archaeology*, 364–380. Oxford: Oxbow Books. DOI: https://doi.org/10.2307/j.ctvh1dk5s.27

Forest, V. 1998. La récente découverte d'une installation de l'Antiquité tardive sur le site d'Ambrussum, Villetelle, Hérault. 2 – Etude des vestiges fauniques. *Revue Archéologique de Narbonnaise*, 31: 217–220. DOI: https://doi.org/10.3406/ran.1998.1506

Forest, V and with the collaboration of **Bardot, A.** 2003. Etude conchyliologique. In: Bouet, A (ed.), "*Thermae Gallicae. Les thermes de Barzan (Charente-Maritime) et les thermes des provinces gauloises*". *Aquitania*, suppl. 11, 479–502. Ausonius: Bordeaux.

Gillikin, DP, Lorrain, A, Bouillon, S, Willenz, P and **Dehairs, F.** 2006. Stable carbon isotopic composition of *Mytilus edulis* shells: relation to metabolism, salinity, $\delta^{13}C$ DIC and phytoplankton. *Organic Geochemistry*, 37: 1371–1382. DOI: https://doi.org/10.1016/j.orggeochem.2006.03.008

Grimstead, DN, Pailes, MC, Dungan, KA, Dettman, DL, Martinez Tagüeña, N and **Clark, AE.** 2013. Identifying the origin of southwestern shell: a geochemical application to Mogollon Rim archaeomolluscs. *American Antiquity*, 78(4): 640–661. DOI: https://doi.org/10.7183/0002-7316.78.4.640

Gruet, Y. 1993. Les coquillages marins : objets archéologiques à ne pas négliger. Quelques exemples d'exploitation et d'utilisation dans l'Ouest de la France. *Revue archéologique de l'ouest*, 10: 157–161. DOI: https://doi.org/10.3406/rao.1993.1005

Harding, JM, Spero, HJ, Mann, R, Herbert, GS and **Sliko, JL.** 2010. Reconstructing early 17th century estuarine drought conditions from Jamestown oysters. *Proceedings of the National Academy of Sciences*, 107(23): 10549–10554. DOI: https://doi.org/10.1073/pnas.1001052107

His, E. 1968. Survie du naissain de *Crassostrea angulata* LMK et *Ostrea edulis* L. à différentes salinités. *Revue des Travaux de l'Institut des P*êches *Maritimes*, 32: 409–412.

Hughes, EH and **Sherr, EB.** 1983. Subtidal food webs in a Georgia estuary: $\delta^{13}C$ analysis. *Journal of Experimental Marine Biology and Ecology*, 67: 227–242. DOI: https://doi.org/10.1016/0022-0981(83)90041-2

Incze, LS, Mayer, LM, Sherr, EB and **Macko, SA.** 1982. Carbon inputs to bivalve mollusks: a comparison of two estuaries. *Canadian Journal of Fisheries and Aquatic Sciences*, 39: 1348–1352. DOI: https://doi.org/10.1139/f82-181

Kirby, MX, Soniat, TM and **Spero, HJ.** 1998. Stable isotope sclerochronology of Pleistocene and recent oyster shells (*Crassostrea virginica*). *Palaios*, 13: 560–569. DOI: https://doi.org/10.2307/3515347

Langlet, D, Alunno-Bruscia, M, de Rafélis, M, Renard, M, Roux, M, Schein, E and **Buestel, D.** 2006. Experimental and natural cathodoluminescence in the shell of *Crassostrea gigas* from Thau lagoon (France): ecological and environmental implications. *Marine*

Ecology Progress Series, 317: 143–156. DOI: https://doi.org/10.3354/meps317143

Lartaud, F. 2007. Les fluctuations haute fréquence de l'environnement au cours des temps géologiques. Mise au point d'un modèle de référence actuel sur l'enregistrement des contrastes saisonniers dans l'Atlantique nord. Ph.D, thesis, UPMC-Paris 06, 336.

Lartaud, F, de Rafélis, M, Ropert, M, Emmanuel, L, Geairon, P and **Renard, M.** 2010c. Mn labelling of living oysters: artificial and natural cathodoluminescence analyses as a tool for age and growth rate determination of *C. gigas* (Thunberg, 1793) shells. *Aquaculture*, 300: 206–217. DOI: https://doi.org/10.1016/j.aquaculture.2009.12.018

Lartaud, F, Emmanuel, L, de Rafélis, M, Pouvreau, S, and **Renard, M.** 2010a. Influence of food supply on the $\delta^{13}C$ signature of mollusc shells: implications for palaeoenvironmental reconstitutions. *Geo-Marine Letters*, 30: 23–34. DOI: https://doi.org/10.1007/s00367-009-0148-4

Lartaud, F, Emmanuel, L, de Rafélis, M, Ropert, M, Labourdette, N, Richardson, CA and **Renard, M.** 2010b. A latitudinal gradient of seasonal teperature variation recorded in oyster shells from the coastal waters of France and The Netherlands. *Facies*, 56: 13. DOI: https://doi.org/10.1007/s10347-009-0196-2

Leng, MJ and **Lewis, JP.** 2016. Oxygen isotopes in Molluscan shell: applications in environmental archaeology. *Environmental Archaeology*, 21(3): 295–306. DOI: https://doi.org/10.1179/1749631414Y.0000000048

Lugand, M and **Bermond, I.** 2001. Carte Archéologique de la Gaule : Agde et le Bassin de Thau, 34/2. Paris: Académie des Inscriptions et Belles-Lettres – Maison des Sciences de l'Homme.

Luterbacher, J, Werner, J-P, Smerdon, J-E, Fernandez-Donado, L, Gonzales-Rouco, J-F, Barriopedro, D, Ljungqvist, F-C, Buntgen, U, Zorita, E, et al. 2016. European summer temperatures since Roman Times. *Environmental Research Letters*, 11: 024001. DOI: https://doi.org/10.1088/1748-9326/11/2/024001

Manca, L. 2014. The individuation of a new type of shell tools during Early Chalcolithic in Sardinia: the bevelled tools on oyster valves. In: Mărgărit, M, Le Dosseur, G and Averbouh, A (eds.), *An experimental approach to reconstruct the operational sequences. An overview of the exploitation of hard animal materials during the neolithic and chalcolithic = O privire asupra exploatării materiilor dure animale de-a lungul neoliticului şi calcoliticului*. Proceedings of the GDRE Prehistos Work-Session: Târgovişte, 5–9 November 2013, 155–182. Târgovişte: Cetatea de Scaun.

Marchand, G, Dupont, C, Laforge, M, Le Bannier, J-C, Netter, C, Nukushina, D, Onfray, M, Querré, G, Quesnel, L and **Stéphan, P.** 2018. *Journal of Archaeological Science: Reports*, 18: 973–983. DOI: https://doi.org/10.1016/j.jasrep.2017.07.014

Marteil, L. 1960. Ecologie des huîtres du Morbihan, *Ostrea edulis* Linné et *Gryphaea angulata* Lamarck. *Revue des Travaux de l'Institut des P*êches *Maritimes*, 24: 335–446.

McConnaughey, TA and **Gillikin, DP.** 2008. Carbon isotopes in mollusc shell carbonates. In: Gröcke, DR and Gillikin, DP (eds.), *Advances in mollusc sclerochronology and sclerochemistry: tools for understanding climate and environment. Geo-Marine Letters*, 28(SI): 287–299. DOI: https://doi.org/10.1007/s00367-008-0116-4

McCrea, JM. 1950. On the isotopic chemistry of carbonates and a paleotemperature scale. *Journal of Chemical Physics*, 18: 849–857. DOI: https://doi.org/10.1063/1.1747785

McElderry, JH. 1963. Mediterranean Tides and Currents. *Irish Astronomical Journal*, 6: 12.

MolluscaBase. 2019a. MolluscaBase. *Mytilaster marioni* (Locard, 1889). Accessed through: World Register of Marine Species. Available at: http://marinespecies.org/aphia.php?p=taxdetails&id=140477 [last accessed 01 April 2019].

MolluscaBase. 2019b. MolluscaBase. *Cerastoderma Poli*, 1795. Accessed through: World Register of Marine Species. Available at: http://www.marinespecies.org/aphia.php?p=taxdetails&id=137735 [last accessed 03 April 2019].

Mouchi, V, Briard, J, Gaillot, S, Argant, T, Forest, V and **Emmanuel, L.** 2018. Reconstructing environments of collection site from archaeological bivalve shells: case study from oysters (Lyon, France). *Journal of Archaeological Science: Reports*, 21: 1225–1235. DOI: https://doi.org/10.1016/j.jasrep.2017.10.025

Pfister, L, Grave, C, Beisel, J-N and **McDonnell, JJ.** 2019. A global assessment of freshwater mollusc shell oxygen isotope signatures and their relation to precipitation and stream water. *Scientific Reports*, 9: 4312. DOI: https://doi.org/10.1038/s41598-019-40369-0

Pierre, C. 1999. The oxygen and carbon isotope distribution in the Mediterranean water masses. *Marine Geology*, 153: 41–55. DOI: https://doi.org/10.1016/S0025-3227(98)00090-5

Py, M. 1993. Dictionnaire des céramiques antiques en Méditerranée nord-occidentale. *Lattara*, 6. Lattes.

Ridout-Sharpe, J. 2017. Shell ornaments, icons and other artefacts from the eastern Mediterranean and Levant. In: Allen, MJ (ed.), *Molluscs in Archaeology*, 290–307. Oxford: Oxbow Books. DOI: https://doi.org/10.2307/j.ctvh1dk5s.23

Riera, P and **Richard, P.** 1996. Isotopic determination of food sources of *Crassostrea gigas* along a trophic gradient in the estuarine bay of Marennes-Oléron. *Estuarine, Coastal and Shelf Science*, 42: 347–360. DOI: https://doi.org/10.1006/ecss.1996.0023

Rivalan, A, Carrato, C, Constant, D, Devillers, B, Forest, V, Sanz, S and **Yung, F.** 2017. Le site antique de Mermian (Agde, Hérault) – Enrochement et amas d'amphore antique dans le fleuve Hérault. Rapport

de fouille – Campagne de sondage – Décembre 2016. Association IBIS – UMR CNRS 5140.

Sharp, Z. 2007. *Principles of stable isotope geochemistry*. Upper Saddle River, NJ: Pearson Prentice Hall.

Surge, D and **Lohmann, KC.** 2008. Evaluating Mg/Ca ratios as a temperature proxy in the estuarine oyster, *Crassostrea virginica*. *Journal of Geophysical Research*, G02001. DOI: https://doi.org/10.1029/2007JG000623

Szabó, K. 2017. Molluscan shells as raw materials for artefact production. In: Allen, MJ (ed.), *Molluscs in Archaeology*, 308–325. Oxford: Oxbow Books. DOI: https://doi.org/10.2307/j.ctvh1dk5s.24

Tynan, S, Dutton, A, Eggins, S and **Opdyke, B.** 2014. Oxygen isotope records of the Australian flat oyster (*Ostrea angasi*) as a potential temperature archive. *Marine Geology*, 357: 195–209. DOI: https://doi.org/10.1016/j.margeo.2014.07.009

Walther, BD and **Rowley, JL.** 2013. Drought and flood signals in subtropical estuaries recorded by stable isotope ratios in bivalve shells. *Estuarine, Coastal and Shelf Science*, 133: 235–243. DOI: https://doi.org/10.1016/j.ecss.2013.08.032

Waselkov, G. 1987. Shellfish gathering and shell midden archaeology. *Advances in Archaeological Method and Theory*, 10: 93–210. DOI: https://doi.org/10.1016/B978-0-12-003110-8.50006-2

How to cite this article: Mouchi, V, Emmanuel, L, Forest, V and Rivalan, A. 2020. Geochemistry of Bivalve Shells As Indicator of Shore Position of the 2nd Century BC. *Open Quaternary*, 6: 4, pp. 1–15. DOI: https://doi.org/10.5334/oq.65

Submitted: 05 April 2019 **Accepted:** 02 January 2020 **Published:** 24 January 2020

]u[*Open Quaternary* is a peer-reviewed open access journal published by Ubiquity Press. OPEN ACCESS